Volume 56 Number 12 December 2013

ISSN 1674-733X CN 11-5847/TP

中国科学：信息科学

SCIENCE CHINA
Information Sciences

Sponsored by
CHINESE ACADEMY OF SCIENCES
NATIONAL NATURAL SCIENCE FOUNDATION OF CHINA

info.scichina.com
www.springer.com/scp
www.springerlink.com

Special Focus on Metamaterials

Guest Editor: CUI TieJun

SCIENCE CHINA PRESS

Springer

Go To Website

SCIENCE CHINA
Information Sciences

Contents

Vol. 56 No. 12 December 2013

Special Focus on Metamaterials (*Progress of Projects Supported by NSFC*)

RESEARCH PAPER

BRIEF REPORT

SCIENCE CHINA
Information Sciences

Progress of Projects Supported by NSFC
Special Focus

December 2013, Vol. 56 120404:1–120404:9
doi: 10.1007/s11432-013-5037-9

Making structured metals transparent for broadband electromagnetic waves

MENG Chong[1], PENG RuWen[1]*, FAN RenHao[1], HUANG XianRong[2] & WANG Mu[1]

[1] *National Laboratory of Solid State Microstructures and Department of Physics, Nanjing University, Nanjing 210093, China;*
[2] *Advanced Photon Source, Argonne National Laboratory, Argonne, Illinois 60439, USA*

Received July 8, 2013; accepted September 23, 2013

Abstract In this review, we present our recent work on making structured metals transparent for broadband electromagnetic waves by surface plasmons (SPs) or spoof surface plasmons (SSPs). First, we demonstrate that the interference between the localized and propagating SPs plays an important role in the optical transmission through arrays of sub-wavelength holes. The observed phenomena belong to the category of plasmonic Fano effects. Second, we show that the transmission enhancement originates not only from the coupling between the incident light and the excited SPs but also from the coupling among these SPs in multiple nano-aperture stacks. Finally, we demonstrate that metallic plates with narrow slit arrays can become transparent within extremely broad spectral bandwidths, and high transmission efficiency is insensitive to the thickness of the metal. This phenomenon explicitly demonstrates the conversion between light and SPs. These investigations provide guidelines to develop many novel materials and devices, such as transparent conducting panels, antireflective solar cells, and other broadband metamaterials.

Keywords transparent metal structures, broadband transmission, surface plasmons

Citation Meng C, Peng R W, Fan R H, et al. Making structured metals transparent for broadband electromagnetic waves. Sci China Inf Sci, 2013, 56: 120404(9), doi: 10.1007/s11432-013-5037-9

1 Introduction

Making metals transparent for white light, which could achieve various fascinating applications, has been expected for a long period. Bulk metals such as gold and silver are naturally opaque to light because of a large mismatch between the refractive indices of metals and dielectrics. Recently, by creating structured materials, it became possible to design materials with electromagnetic properties extending beyond their natural characteristics. For instance, free electrons may induce surface plasmons (SPs) [1] or spoof surface plasmons (SSPs) in the long-wavelength regime [2] in structured metals. These SPs can propagate along nano-structures such as nano-holes, nano-slit walls, and nano-wires. When SP propagation is blocked by geometric boundaries, the SPs may be converted back into light and thus contribute to optical transmission through the structured metals [3–11]. Related works have generated much interest in the fields of plasmonics [1], surface-enhanced Raman scattering (SERS) [12,13], and so on.

*Corresponding author (email: rwpeng@nju.edu.cn)

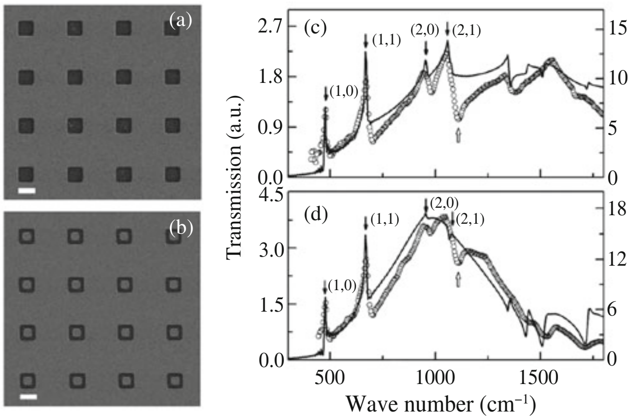

Figure 1   (a), (b) SEM micrographs of arrays of (a) open square apertures and (b) ring-shaped apertures with a central solid square metal patch. The bar denotes a length of 20 μm; (c), (d) the measured and calculated transmission spectra of (c) the open aperture array and (d) the ring-shaped-aperture array. The solid lines are the calculated data and the open circles are the experimental points. The scale for the experimental data is on the left side of the figure, and the scale for the calculated spectra is on the right side (partially adapted from [11]).

Metallic micro- and nano-structures can be used as building blocks to construct metamaterials [14], which have been used in the studies of super-lenses [15,16], negative refraction [17,18], optical magnetism [19–22], high index refraction [23,24], invisibility cloaking [25–27], the manipulation of chirality and polarization [28–31], and many other interesting phenomena that extend beyond the properties of natural materials. However, these metamaterials have some common limitations. One of the limitations is the narrow transmission bandwidths, which typically appear as discrete resonant peaks. Another limitation is that the transmission efficiency is usually low for thick materials. Therefore, increasing the working bandwidth and the transmission efficiency remains a major challenge.

In this review, we present our recent work on making structured metals transparent for broadband electromagnetic waves by surface plasmons (SPs) or spoof surface plasmons (SSPs). First, we demonstrate the interference between localized and propagating SPs and its effect on optical transmission. Second, we show that the transmission enhancement originates not only from the coupling between the incident light and the excited SPs but also from the coupling among these SPs in multiple nano-aperture stacks. Finally, we show that metallic plates with narrow slit arrays can become transparent within extremely broad spectral bandwidths, and high transmission efficiency is insensitive to the thickness of the metal. We expect that these investigations will provide guidelines to develop novel opto-materials and devices.

2   Interference between localized and propagating SPs and its role in the optical transmission through a subwavelength-aperture array

In this section, we show that when the light is incident on a metal surface with a sub-wavelength-aperture array, the phase difference between the propagating and localized SPs can be tuned by the geometrical parameters of the array [11,32,33]. This plasmonic Fano effect eventually affects the optical transmission in sub-wavelength hole systems [11].

Two types of aperture arrays are fabricated on gold films through photolithography. The first type consists of open square apertures (Figure 1(a)). The second type is a square array of ring-shaped apertures (Figure 1(b)). In the case of an open square aperture (Figure 1(a)), four peaks appear (see Figure 1(c)), while in the case of a ring-shaped aperture (Figure 1(b)), some modes are enhanced but some are suppressed (Figure 1(d)). Below the resonance frequency of an individual aperture (ν_0) [11], enhanced transmission (peak) appears at the specific frequencies owing to the constructive interference between the propagating and localized SPs, while above ν_0, suppressed transmission (dip) is observed owing to the destructive interference between those SPs. Thus, by tuning either the aperture configuration or the lattice parameter of the aperture array it is possible to change both the position of transmission

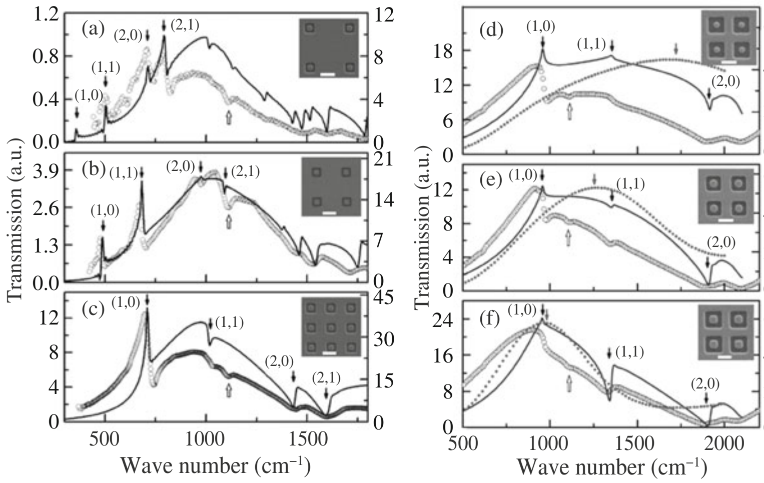

Figure 2 (a)–(c) The measured and calculated transmission spectra of the ring-shaped aperture arrays with different lattice parameters: (a) 8.0 μm, (b) 6.0 μm, and (c) 4.0 μm. Here, the bars in each inset denote a length of 30 μm; (d)–(f) the measured and calculated transmission spectra of the ring-shaped aperture arrays with different central patch sizes: (d) 0.6 μm, (e) 0.8 μm, and (f) 1.0 μm. Here, the lattice parameter and the outer rim of the aperture were kept identical in all cases. The bar in the inset denotes a length of 20 μm. The dotted line illustrates the resonant property of each individual aperture, the resonant frequency of which is marked by the gray arrow. The calculated spectra are indicated by solid lines, and the experimental data are indicated by open circles (partially adapted from [11]).

peaks/dips and the resonance frequency of the individual aperture (ν_0).

As illustrated in Figure 2 (a)–(c), the extrema in the transmission spectra can be changed from peaks to dips and vice versa by adjusting the configuration of the aperture array. The transmission spectra can also be tuned by changing the aperture configuration. For example, if the dimensions of all central square patches are reduced, the resonance frequency of an individual aperture, ν_0, increases. As a result, some dips in previous transmission spectra become peaks (as shown in Figure 2 (d)–(f)).

Therefore, we have demonstrated that when the light is incident on a metal surface perforated with a sub-wavelength-aperture array, the phase difference between the propagating and localized SPs can be tuned using the geometrical parameters of the array, which eventually affect the optical transmission [11,32,33]. Above the resonant frequency of the individual aperture, destructive interference between the two types of SPs leads to the appearance of a minimum in the transmission spectra, while below the resonant frequency of the individual aperture, constructive interference of these SPs leads to the appearance of a maximum. The observed phenomena belong to the category of plasmonic Fano effects. We suggest that this feature of sub-wavelength aperture arrays can be applied to the engineering of surface-wave-based all-optical devices.

3 Coupling of SPs influences the optical transmission in multiple nano-aperture stacks

In this section, we show that the transmission enhancement of light originates not only from the coupling between the incident light and the excited SPs but also from the coupling among these SPs in the Ag/SiO_2 multilayer within a periodic sub-wavelength-aperture array [34,35].

First, we present the optical properties of the silver film with periodic arrays of sub-wavelength apertures, for the following three cases. (1) The silver film is free-standing and the apertures are in vacuum; this case is termed the "A-Ag-A" case. (2) The silver film is sandwiched by the SiO_2 film, and the apertures are also filled with SiO_2; this case is termed the "Q-Ag-Q" case. (3) The silver film is sandwiched between vacuum and SiO_2, and the apertures are in vacuum; this case is termed the "A-Ag-Q" case. When light illuminates these structured silver films, optical transmission and reflection can be calculated by using the full vectorial three-dimensional (3D) finite-difference time-domain (FDTD) method. Fig-

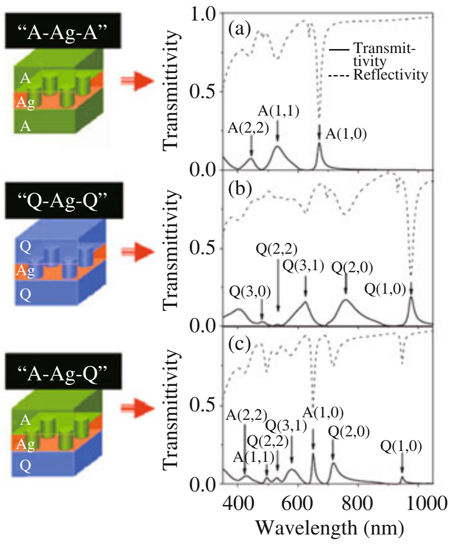

Figure 3 The FDTD calculated transmission and reflection spectra of the structured silver films at normal incidence. (a) The "A-Ag-A" case, i.e., the silver film is free-standing and the apertures are in vacuum; (b) the "Q-Ag-Q" case, i.e., the silver film is sandwiched by SiO_2 films and the apertures are also filled with SiO_2; (c) the "A-Ag-Q" case, i.e., the silver film is sandwiched between vacuum and SiO_2 and the apertures are in vacuum. Each structure has a 100-nm-thick silver layer, an aperture array of periodicity 600 nm, and apertures of diameter 150 nm (partially adapted from [34]).

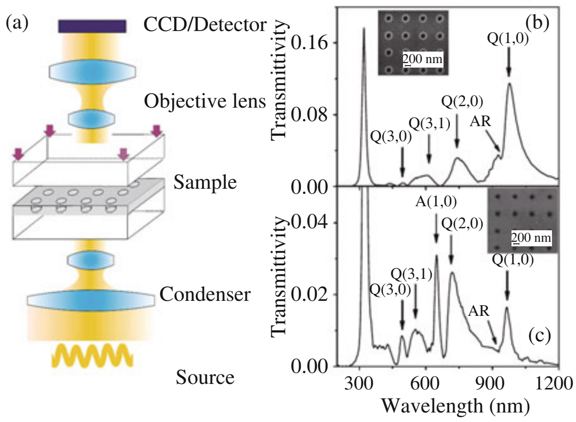

Figure 4 (a) A schematic setup for optical measurements; (b), (c) the measured transmission spectra of structured silver films at normal incidence: (b) the "Q-Ag-Q" case, and (c) the "A-Ag-Q" case. The scanning electronic microscope (SEM) images of two samples are given in the insets. Each sample has a 100-nm-thick silver layer, an aperture array of periodicity 600 nm, and apertures of diameter 150 nm. Main peaks are indexed by two integers and the dips are marked by "AR" (partially adapted from [34,35]).

ure 3 illustrates the transmission and reflection spectra obtained at the normal incidence for three types of films considered above. Transmission peaks and reflection dips can be clearly identified at optical frequencies.

It is of interest to note that in a dielectric/structured metal/dielectric sandwich, the SPs on one metal-dielectric interface may couple with those on the other interface. If the SPs on both interfaces belong to the same mode, their coupling will lead to the enhancement of the transmission. If, however, the SPs on different interfaces belong to different modes, their coupling will result in a blue shift of the transmission modes. Owing to the fact that the coupling of SPs is influenced by the thickness of the metallic film, the extent of the blue shift of the transmission peak depends on the thickness of the metallic film [34]. The experimental results shown in Figure 4 are in good agreement with the results of numerical calculations.

Now, we focus on how the coupling of SPs influences the optical transmission in multiple nano-aperture stacks. A multiple nano-aperture stack is constructed by defining the following two layers as a building block: one layer is a silver film with a periodic array of sub-wavelength SiO_2 holes; the other is a film of SiO_2. Figure 5 illustrates a schematic of nano-structured Ag/SiO_2 multilayer films and their experimental and calculated optical transmission spectra. Two interesting features are observed. First, by increasing the repeating number of building blocks, new resonant modes may be obtained in the transmission spectra. Second, the quality factor of the transmission peak can be significantly increased by increasing the number of building blocks. These features may originate from multiple scatterings and also the coupling effect of light waves in multilayer systems.

In order to illustrate multiple scatterings of electromagnetic wave and also the coupling effect in the multilayer structure, we have calculated the electric-field distribution of mode Q(3,1) in several multilayer structures, as shown in Figure 6. It is clearly indicated that the coupling of SPs possesses collective behavior and dramatically influences the optical transmission through the multilayers

Therefore, we have demonstrated that the enhancement of optical transmission originates not only from the coupling between the incident light and excited SPs but also from the coupling among excited SPs in multiple nano-aperture stacks [34,35]. The coupling of SPs is strongly dependent of the detailed

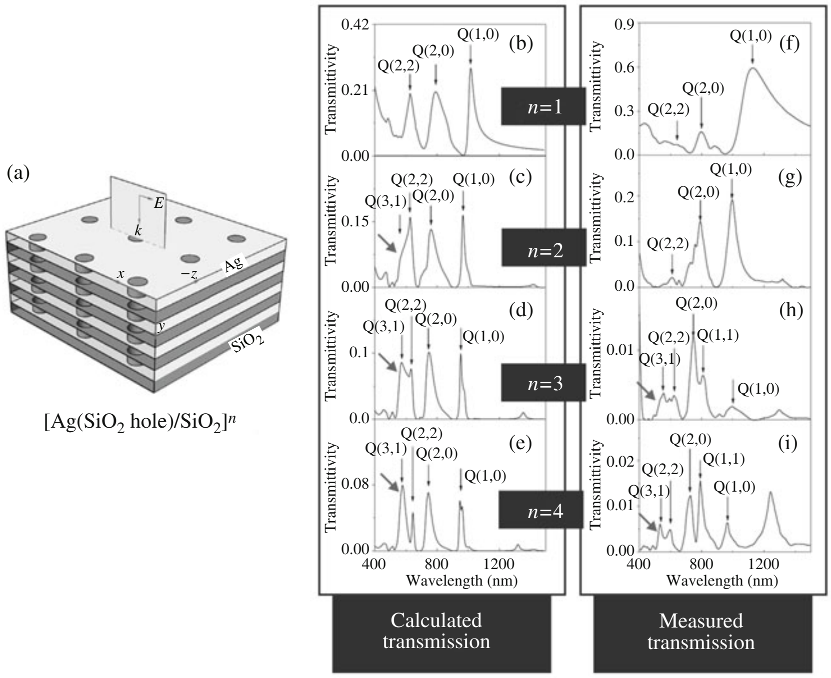

Figure 5 (a) A schematic of a nano-structured Ag/SiO_2 multilayer film; (b)–(i) the FDTD calculated and experimentally measured transmission spectra of samples with: (b) and (f) $n = 1$ and $t = 100$ nm; (c) and (g) $n = 2$ and $t = 200$ nm; (d) and (h) $n = 3$ and $t = 300$ nm; (e) and (i) $n = 4$ and $t = 400$ nm, where n is the repeating number of building blocks and t is the total thickness of the film. Each building block contains two layers: a 50-nm-thick SiO_2 layer and a 50-nm-thick silver film with a periodic sub-wavelength aperture array. The lattice parameter of the aperture array is 600 nm, and the diameters of apertures are 150 nm. The incident light is normal to the film (partially adapted from [34]).

nanostructure of a film. In a structured metal–dielectric sandwich, the coupling of SPs can cause a shift of transmission peaks, which dramatically decreases when the thickness of the silver film is increased. On the other hand, in the nanostructured metal–dielectric multilayers, the coupling of SPs can induce new resonant modes and increase the quality factors of transmission peaks. Physically these properties originate from multiple scatterings and the coupling effect of light waves in these structures. We suggest that these features may have potential applications in the design of subwavelength optoelectronic materials and devices.

4 Making structured metals transparent for broadband electromagnetic waves by surface plasmons or spoof surface plasmons

We now describe the attempts to expand the spectral bandwidth of operation and increase the efficiency of transmission for applications. In this section, we demonstrate that metallic gratings with narrow slits can become non-dispersively transparent to broadband electromagnetic waves [6,7].

As is known, a one-dimensional metallic grating (Figure 7(a)) is one of the simplest plasmonic metamaterials. Let us define the grating period, the grating thickness, and the slit width as d, τ, and W, respectively. It is found that when light is incident on the metallic grating in an angular range of oblique incidence, the grating becomes transparent to TM polarization in the entire long-wavelength region (Figure 7(b)). This phenomenon of broadband transmission can be understood at the microscopic level (Figure 7). The incident wave drives the free electrons on the metallic surfaces and a part of the slit walls to form SPs (or SSPs). These excited SPs (or SSPs) propagate along the slit walls but are blocked by the bottom edges, forming oscillating positive and negative charges. The oscillating charges eventually emit the transmitted wave. The transmission efficiency reaches a maximum [6] at an optimal incidence angle of $\theta_f \approx \arctan(d/W - 1)$.

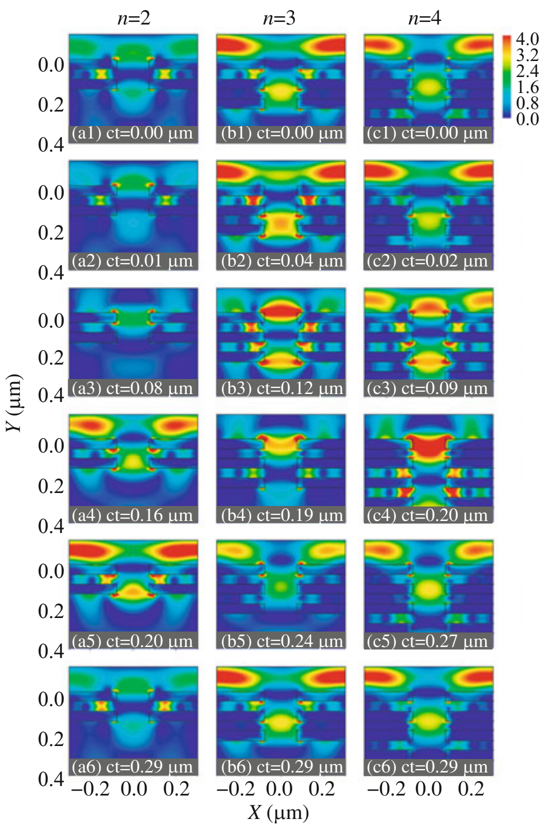

Figure 6 The calculated electric-field distribution of the Q(3,1) mode in several nano-structured multilayer films, in which the TM-polarized light illuminates the multilayer from top to bottom. In one temporal period, the electric-field distributions of the Q(3,1) mode are shown in the multilayer film for: (a1)–(a6) $n = 2$, (b1)–(b6) $n = 3$, and (c1)–(c6) $n = 4$. Here, n represents the repeating number of building blocks in the multilayer, t is the time in a temporal period, and c is the speed of light in vacuum (adapted from [34]).

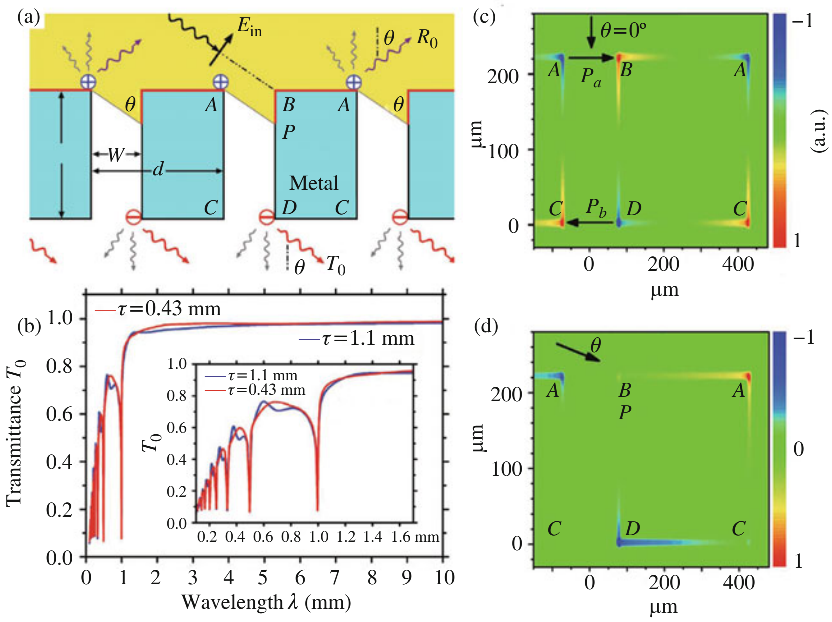

Figure 7 (a) The schematic of light tunneling by driving the free electrons on the metallic surfaces and slit walls; (b) the calculated transmission spectra of TM-polarized light passing through two gold gratings with the same period $d = 0.5$ mm, the same slit width $W = 0.05$ mm, but different thicknesses ($\tau = 0.43$ mm (red curve) and $\tau = 1.1$ mm (blue curve)), at the optimal angle of incidence. The transmission spectra in the shorter wavelength range are shown in the inset, where the sharp transmission dips arise from Wood anomalies. The typical charge-density distributions, calculated at the high-transmission region: (c) normal incidence, and (d) optimal incidence with θ_f (partially adapted from [7]).

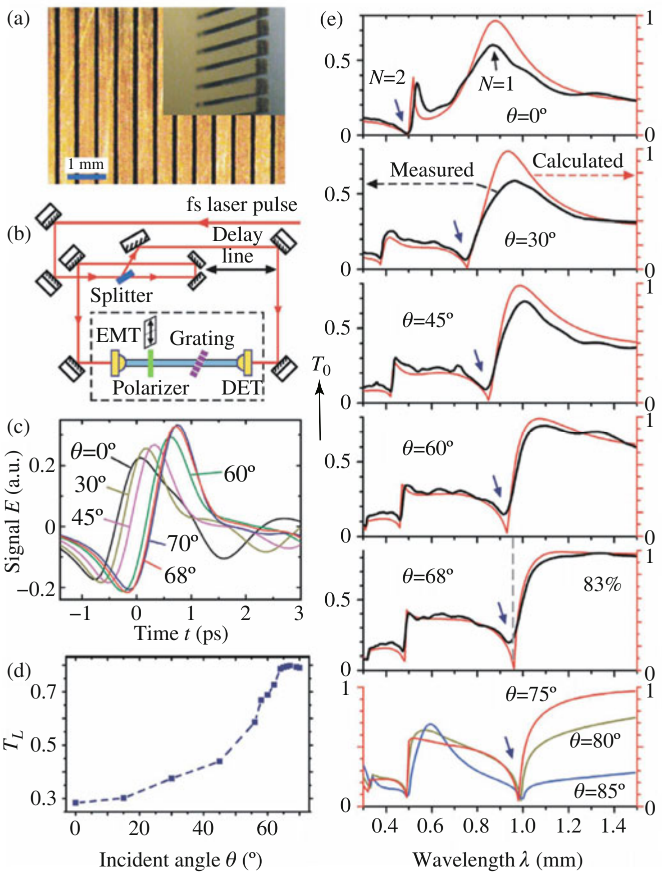

Figure 8 (a) Optical image of the metal grating with $d = 0.5$ mm, $W = 0.15$ mm, and $\tau = 0.34$ mm. The inset illustrates the cross-section; (b) schematic setup for experimental measurements in the THz regime, where EMT represents the THz emitter, DET represents the THz detector, and the dashed-line box is an N_2 purging box; (c) the measured time-domain THz transmission signals at different incident angles of the THz wave. (d) Average transmission efficiency for wavelengths in the range of 1.05 mm $\leqslant \lambda \leqslant$ 1.5 mm. (e) The measured and the calculated transmission spectra. Note that the spectral region in which the strong and flat broadband transmission occurs corresponds to the wavelengths larger than the 1st Wood anomaly, marked by a navy-blue arrow (adapted from [7]).

In the experiments, we have fabricated different metallic gratings for transmission measurements in the terahertz (THz) frequency range. As shown in Figure 8, Fabry-Perot resonances are observed at normal incidence. However, at oblique incidence, the long-wavelength transmission increases gradually as the angle of incidence (θ) is increased. At $\theta = 68°$, transmittance becomes significantly strong and nearly flat in the whole range of wavelengths satisfying $\lambda > \lambda_{\rm WD1}$ (where $\lambda_{\rm WD1}$ corresponds to the first-order Wood anomaly), and the values of transmission efficiency reach $T_0 \sim 83\%$ (measured) and 99% (calculated). Therefore, we confirmed that metallic gratings become highly transparent to ultra-broadband long-wavelength electromagnetic waves at oblique incidence. Additional experiments [7] indicate that the ultra-broadband transmission is insensitive to the grating thickness, but the Fabry-Perot resonance sensitively depends on the thickness.

Therefore, metallic gratings with narrow slits can become highly transparent for ultra-broad bandwidths at oblique incidence [6,7]. The ultrabroadband optical transmission is verified both experimentally and theoretically for the structured metals with significant thickness. Interestingly, the transmission efficiency is insensitive to the thickness of metal. These metal gratings then possess both advantages: high-efficiency transmission and high-performance electrical properties. Our investigations have demonstrated a simple yet efficient way to make ultrabroadband transparent metals, and also to achieve the applications on stealth technologies and antireflection solar cells, etc. The underlying physics may also shed new light on widening the spectral bandwidths and increasing of the efficiency of more complicated artificial materials, including acoustic metamaterials [36].

5 Conclusion

In this paper, we review our recent work on making structured metals transparent for broadband electromagnetic waves by SPs (or SSPs). First, we have demonstrated the interference between localized and propagating SPs and its effect on the optical transmission through subwavelength-hole arrays [11,32,33], which belongs to plasmonic Fano effects. Second, we have presented that the enhancement of optical transmission originates not only from the coupling between the incident light and the excited SPs, but also from the coupling among those SPs in multiple nanoaperture stacks [34,35]. Third, we have demonstrated that the metallic plates with narrow slit arrays can become transparent for ultra-broad spectral bandwidths, and high transmission efficiency is insensitive to the metal thickness [6,7]. The conversion between light and SPs is explicitly presented in the observed phenomena. The investigations provide a guideline to develop many novel materials and devices, including transparent conducting panels, antireflective solar cells, white-beam polarizers, and other broadband metamaterials.

Finally, it is worthwhile to emphasize that some alternative resonant or non-resonant mechanisms have been developed to make metals transparent. For example, Zhou et al. have achieved a transparent but continuous (apertureless) metal film via the scattering cancellation mechanism [37,38]. Shuang and coauthors [39] have demonstrated electromagnetically induced transparency (EIT) in metamaterials. These works have also significantly contributed to a rapid advancement in transparent structured metals. The investigations are achieving applications in the areas such as plasmonics, SERS, and metamaterials.

Acknowledgements

This work was financially supported by Ministry of Science and Technology of China (Grant Nos. 2012CB921502, 2010CB630705), and National Science Foundation of China (Grant Nos. 11034005, 61077023). Huang X R was supported by the US Department of Energy, Office of Science, Office of Basic Energy Sciences (Contract No. DE-AC-02-06CH11357).

References

1 Barnes W L, Dereux A, Ebbesen T W. Surface plasmon subwavelength optics. Nature, 2003, 424: 824–830
2 Pendry J B, Martín-Moreno L, García-Vidal F J. Mimicking surface plasmons with structured surfaces. Science, 2004, 305: 847–848
3 Ebbesen T W, Lezec H J, Ghaemi H F, et al. Extraordinary optical transmission through sub-wavelength hole arrays. Nature, 1998, 391: 667–669
4 Porto J A, García-Vidal F J, Pendry J B. Transmission resonances on metallic gratings with very narrow slits. Phys Rev Lett, 1999, 83: 2845–2848
5 Liu H, Lalanne P. Microscopic theory of the extraordinary optical transmission. Nature, 2008, 452: 728–731
6 Huang X R, Peng R W, Fan R H. Making metals transparent for white light by spoof surface plasmons. Phys Rev Lett, 2010, 105: 243901
7 Fan R H, Peng R W, Huang X R, et al. Transparent metals for ultrabroadband electromagnetic waves. Adv Mater, 2012, 24: 1980–1986
8 Alù A, D'Aguanno G, Mattiucci N, et al. Plasmonic brewster angle: broadband extraordinary transmission through optical gratings. Phys Rev Lett, 2011, 106: 123902
9 Subramania G, Foteinopoulou S, Brener I. Nonresonant broadband funneling of light via ultrasubwavelength channels. Phys Rev Lett, 2011, 107: 163902
10 Hooper I R, Preist T W, Sambles J R. Making tunnel barriers (including metals) transparent. Phys Rev Lett, 2006, 97: 053902
11 Bao Y J, Peng R W, Shu D J, et al. Role of interference between localized and propagating surfacewaves on the extraordinary optical transmission through a subwavelength-aperture array. Phys Rev Lett, 2008, 101: 087401
12 Xu H X, Bjerneld E J, Käll M, et al. Spectroscopy of single Hemoglobin molecules by surface enhanced raman scattering. Phys Rev Lett, 1999, 83: 4357–4360
13 Xu H X, Wang X H, Persson M P, et al. Unified treatment of fluorescence and Raman scattering processes near metal surfaces. Phys Rev Lett, 2004, 93: 243002
14 Liu Y M, Zhang X. Metamaterials: a new frontier of science and technology. Chem Soc Rev, 2011, 40: 2494–2507
15 Pendry J B. Negative refraction makes a perfect lens. Phys Rev Lett, 2000, 85: 3966–3969

16 Zhang X, Liu Z. Superlenses to overcome the diffraction limit. Nat Mat, 2008, 7: 435–441
17 Shelby R A, Smith D R, Schultz S. Experimental verification of a negative index of refraction. Science, 2001, 292: 77–79
18 Valentine J, Zhang S, Zentgraf T, et al. Three-dimensional optical metamaterial with a negative refractive index. Nature, 2008, 455: 376–379
19 Pendry J B, Holden A J, Robbins D J, et al. Magnetism from conductors and enhanced nonlinear phenomena. IEEE Trans Microwave Theory Tech, 1999, 47: 2075–2084
20 Yen T J, Padilla W J, Fang N, et al. Terahertz magnetic response from artificial materials. Science, 2004, 303: 1494–1496
21 Linden S, Enkrich C, Wegener M, et al. Magnetic response of metamaterials at 100 terahertz. Science, 2004, 306: 1351–1353
22 Xiong X, Sun W H, Bao Y J, et al. Switching the electric and magnetic responses in a metamaterial. Phys Rev B, 2009, 80: 201105(R)
23 Shen J T, Catrysse P B, Fan S. Mechanism for designing metallic metamaterials with a high index of refraction. Phys Rev Lett, 2005, 94: 197401
24 Choi M, Lee S H, Kim Y, et al. A terahertz metamaterial with unnaturally high refractive index. Nature, 2011, 470: 369–373
25 Pendry J B, Schurig D, Smith D R. Controlling electromagnetic fields. Science, 2006, 312: 1780–1782
26 Ma H F, Cui T J. Three-dimensional broadband ground-plane cloak made of metamaterials. Nat Commun, 2010, 1: 21
27 Zhao J Z, Wang D L, Peng R W, et al. Watching outside while under a carpet cloak of invisibility. Phys Rev E, 2011, 84: 046607
28 Zhang S, Park Y S, Li J. Negative refractive index in chiral metamaterials. Phys Rev Lett, 2009, 102: 023901
29 Hao J, Yuan Y, Ran L, et al. Manipulating electromagnetic wave polarizations by anisotropic metamaterials. Phys Rev Lett, 2007, 99: 063908
30 Zhang S, Wei H, Bao K, et al. Chiral surface plasmon polaritons on metallic nanowires. Phys Rev Lett, 2011, 107: 096801
31 Xiong X, Sun W H, Bao Y J. Construction of a chiral metamaterial with a U-shaped resonator assembly. Phys Rev B, 2010, 81: 075119
32 Bao Y J, Zhang B, Wu Z, et al. Surface-plasmon-enhanced transmission through metallic film perforated with fractal-featured aperture array. Appl Phys Lett, 2007, 90: 251914
33 Bao Y J, Li H M, Chen X C, et al. Tailoring the resonances of surface plasmas on fractal-featured metal film by adjusting aperture configuration. Appl Phys Lett, 2008, 92: 151902
34 Tang Z H, Peng R W, Wang Z, et al. Coupling of surface plasmons in nanostructured metal/dielectric multilayers with subwavelength hole arrays. Phys Rev B, 2007, 76: 195405
35 Gao F, Li D, Peng R W, et al. Tunable interference of light behind subwavelength apertures. Appl Phys Lett, 2009, 95: 011104
36 Qi D X, Fan R H, Peng R W, et al. Multiple-band transmission of acoustic wave through metallic gratings. Appl Phys Lett, 2012, 101: 061912
37 Zhou L, Wen W J, Chan C T, et al. Electromagnetic-wave tunneling through negative-permittivity media with high magnetic fields. Phys Rev Lett, 2005, 94: 243905
38 Song Z Y, He Q, Xiao S Y, et al. Making a continuous metal film transparent via scattering cancellations. Appl Phys Lett, 2012, 101: 181110
39 Zhang S, Genov D A, Wang Y, et al. Plasmon-induced transparency in metamaterials. Phys Rev Lett, 2008, 101: 047401

Information for authors

SCIENCE CHINA Information Sciences (Sci China Inf Sci), cosponsored by the Chinese Academy of Sciences and the National Natural Science Foundation of China, and published by Science China Press, is committed to publishing high-quality, original results of both basic and applied research in all areas of information sciences, including computer science and technology; systems science, control science and engineering (published in Issues with odd numbers); information and communication engineering; electronic science and technology (published in Issues with even numbers). Sci China Inf Sci is published monthly in both print and electronic forms. It is indexed by Academic OneFile, Astrophysics Data System (ADS), CSA, Cabells, Current Contents/Engineering, Computing and Technology, DBLP, Digital Mathematics Registry, Earthquake Engineering Abstracts, Engineering Index, Engineered Materials Abstracts, Gale, Google, INSPEC, Journal Citation Reports/Science Edition, Mathematical Reviews, OCLC, ProQuest, SCOPUS, Science Citation Index Expanded, Summon by Serial Solutions, VINITI, Zentralblatt MATH.

Papers published in *Sci China Inf Sci* include:

REVIEW (20 printed pages on average) surveys representative results and important advances on well-identified topics, with analyses and insightful views on the states of the art and highlights on future research directions.

RESEARCH PAPER (no more than 15 printed pages) presents new and original results and significant developments in all areas of information sciences for broad readership.

BRIEF REPORT (no more than 4 printed pages) describes key ideas, methodologies, and results of latest developments in a timely manner.

Authors are recommended to use *Science China*'s online submission services. To submit a manuscript, please go to www.scichina.com, create an account to log in http://mco3.manuscriptcentral.com/scis, and follow the instructions there to upload text and image/table files.

Authors are encouraged to submit such accompanying materials as short statements on the research background and area/subareas and significance of the work, and brief introductions to the first and corresponding authors including their mailing addresses with post codes, telephone numbers, fax numbers, and e-mail addresses. Authors may also suggest several qualified experts (with full names, affiliations, phone numbers, fax numbers, and e-mail addresses) as referees, and/or request the exclusion of some specific individuals from potential referees.

All submissions will be reviewed by referees selected by the editorial board. The decision of acceptance or rejection of a manuscript is made by the editorial board based on the referees' reports. The entire review process may take 90 to 120 days, and the editorial office will inform the author of the decision as soon as the process is completed. If the editorial board fails to make a decision within 120 days, please contact the editorial office.

Authors should guarantee that their submitted manuscript has not been published before and has not been submitted elsewhere for print or electronic publication consideration. Submission of a manuscript is taken to imply that all the named authors are aware that they are listed as coauthors, and they have agreed on the submitted version of the paper. No change in the order of listed authors can be made without an agreement signed by all the authors.

Once a manuscript is accepted, the authors should send a copyright transfer form signed by all authors to Science China Press. Authors of one published paper will be presented one sample copy. If more sample copies or offprints are required, please contact the managing editor and pay the extra fee. The full text opens free to domestic readers at www.scichina.com, and is available to overseas readers at www.springerlink.com.

Subscription information

ISSN print edition: 1674-733X
ISSN electronic edition: 1869-1919
Volume 56 (12 issues) will appear in 2013

Subscription rates
For information on subscription rates please contact:
Customer Service
China: sales@scichina.org
North and South America:
journals-ny@springer.com
Outside North and South America:
subscriptions@springer.com

Orders and inquiries:
China
Science China Press
16 Donghuangchenggen North Street, Beijing 100717, China
Tel: +86 10 64015683
Fax: +86 10 64016350
Email: informatics@scichina.org
North and South America
Springer New York, Inc.
Journal Fulfillment, P.O. Box 2485
Secaucus, NJ 07096 USA
Tel: 1-800-SPRINGER or 1-201-348-4033
Fax: 1-201-348-4505
Email: journals-ny@springer.com
Outside North and South America:
Springer Distribution Center
Customer Service Journals
Haberstr. 7, 69126 Heidelberg, Germany
Tel: +49-6221-345-0, Fax: +49-6221-345-4229
Email: subscriptions@springer.com

Cancellations must be received by September 30 to take effect at the end of the same year.

Changes of address: Allow for six weeks for all changes to become effective. All communications should include both old and new addresses (with postal codes) and should be accompanied by a mailing label from a recent issue. According to § 4 Sect. 3 of the German Postal Services Data Protection Regulations, if a subscriber's address changes, the German Federal Post Office can inform the publisher of the new address even if the subscriber has not submitted a formal application for mail to be forwarded. Subscribers not in agreement with this procedure may send a written complaint to Customer Service Journals, Karin Tiks, within 14 days of publication of this issue.

Microform editions are available from: ProQuest. Further information available at http://www.il.proquest.com/uni

Electronic edition
An electronic version is available at springerlink.com.

Production
Science China Press
16 Donghuangchenggen North Street, Beijing 100717, China
Tel: +86 10 64015683 or +86 10 64034134
Fax: +86 10 64016350
Printed in the People's Republic of China
Jointly published by
Science China Press and Springer

ISSN 1674-733X